Chapter 7

Nanostructured Si/SiO_2 Quantum Wells

Toshio Takeuchi and Yoshiji Horikoshi

Additional information is available at the end of the chapter

http://dx.doi.org/10.5772/intechopen.79880

Abstract

The motivation for developing light-emitting devices on an indirect transition semiconductor such as silicon has been widely discussed for Si/SiO_2 nanostructures. In this chapter, we report on the fabrication of Si/SiO_2 quantum-confined amorphous nanostructured films and their optical properties. The Si/SiO_2 nanostructures comprising amorphous Si, SiO_2, and Si/SiO_2 multilayers are grown using ultrahigh vacuum radio frequency magnetron sputtering. Optical absorption coefficients of the Si/SiO_2 nanostructures are evaluated with regard to tentative integrated Si thicknesses. Optical energy band gaps of the Si/SiO_2 multilayer films are in accordance with the effective mass theory and described as $E_0 = 1.61 + 0.75d^{-2}$ eV at the Si layer-integrated thicknesses ranging from 0.5 to 6 nm. Quantum confinement effects in the Si/SiO_2 nanostructures are inferred from optical transmittance and reflectance spectra. The rapid-thermal-annealed Si/SiO_2 multilayer films demonstrate the intensified photoluminescence at ~1.45 eV due to the formation of nanocrystalline silicon. The temperature dependence of the nanocrystalline luminescence intensity shows the nonmonotonous behavior which is interpreted invoking the Kapoor model.

Keywords: amorphous Si/SiO_2, quantum confinement, nanocrystals, optical properties, absorption coefficient, photoluminescence, the Kapoor model

1. Introduction

Silicon, the principal semiconducting material, inherits the indirect optical transitions from its band structure. The research efforts are put forth on realization of light emission effects in silicon-based Si/SiO_2 nanostructured devices exploring hydrogenated amorphous Si [1–9], porous Si [10–12], Si quantum dots [13–19], amorphous Si quantum wells (QWs) [20–24], crystalline and nanocrystalline Si QWs [25–28], and Er-doped QWs [29–31]. The fabrication of Si/SiO_2 QWs has been an attractive area in process technology of Si-based light-emitting devices

in last few decades. Various techniques are developed to synthesize the Si/SiO_2 nanostructured films—molecular beam epitaxy (MBE) [32–37], plasma-enhanced chemical vapor deposition (PECVD) [38–49], magnetron sputtering [50–65], electrochemical dissolution in electrolytes, ion implantation, and others. In this chapter, we investigate the growth of amorphous Si/SiO_2 QWs employing an ultrahigh vacuum (UHV) radio frequency (RF) magnetron sputtering (MS) system. This method is simple and easy to use in a manual operation. The Si/SiO_2 QW films are fabricated on sapphire and silicon wafers at room temperature to enable the atomic precision of the film growth via minimization of atomic movements during and after the depositions. Morphology, crystallinity, atomic bonding, and structures of the Si/SiO_2 films are evaluated by means of focused-ion-beam scanning electron microscopy (FIB-SEM), X-ray diffraction (XRD), and high-resolution X-ray photoelectron spectroscopy (XPS). The Si/SiO_2 films are distinguished with the layer number (the period), the Si thickness (the QW thickness), and the SiO_2 thickness (the barrier thickness). The first identification of the quantum confinement effects is made speculating on the optical energy band gap determined from the optical absorption and reflectance measurements taking into account the energy band gaps of silicon and fused quartz as ~1.1 and ~7.8 eV, respectively. To minimize the experimental uncertainty, the Si/SiO_2 films are deposited at room temperature. At the raised temperature conditions, the uncertainty remains the atomic diffusion, reactions, and oxidation at the Si/SiO_2 interface. On the other hand, the deposited Si and SiO_2 layers are expected as in amorphous conditions. At first, we restricted the Si/SiO_2 nanostructured layer films to be amorphous. Photoluminescence (PL) is used to characterize the as-grown and annealed materials. The thermal annealing is expected to improve the photoluminescence characteristics.

2. Experiment

2.1. Si/SiO_2 layer films preparation

Si/SiO_2 QWs films are synthesized in an ultrahigh vacuum (UHV; 3×10^{-8} Pa) RF MS system at a very small deposition rate (from 0.005 to 0.5 nm/s). The schematics of the UHV RF magnetron sputtering systems are shown in **Figure 1**. The ultrahigh vacuum chamber is equipped with two AJA A300 UHV RF magnetron sputtering guns connected to argon and oxygen gas lines, sputter ion guns, and 5 N Si and 5 N fused quartz SiO_2 targets. Preparation temperatures are controlled at the substrate holder. Transparent substrates are used for optical measurements; crystalline and amorphous substrates are used to test the influence of substrate crystallinity on the film growth. All depositions are operated at room temperature on both transparent sapphire A and opaque Si (100) substrates. The polished sapphire substrates are etched in dilute HF and put into the UHV chamber. The base pressure of the chamber is 10^{-7} Pa, and the sputtering gun pressure during the plasma operation in argon is 2×10^{-1} Pa. The deposition process is a repetition of Si and SiO_2 depositions separated by an interval time. The deposition parameters of the quantum-well structures are the well layer thickness, the barrier layer thickness, and the number of periodicity. The thickness of each layer is controlled by the deposition speed and the sputtering time. Basic deposition speeds are 0.05 nm/s for Si and

http://dx.doi.org/10.5772/intechopen.79880

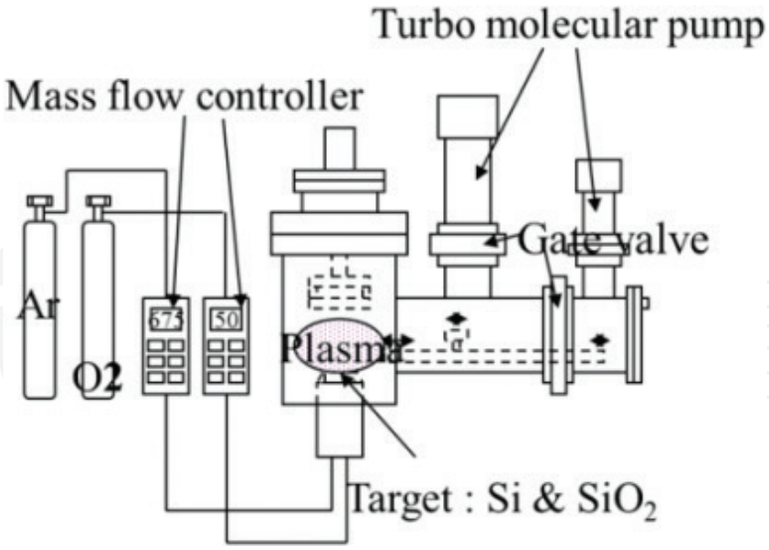

Figure 1. A schematic drawing of the ultrahigh vacuum radio frequency magnetron sputtering. Sputtering targets can be changed at each deposition program.

0.021 nm/s for SiO_2 at an argon pressure of 0.2 Pa. Minimization of the atomic diffusion and the oxidation during the depositions are the main concerns. The Si/SiO_2 nanostructure films are made of 1–50 periods consisting of 0.5–15 nm thick Si QWs and 0.5–6 nm thick SiO_2 barriers. The 10-layer Si/SiO_2 nanostructured layers are formed with the total thickness of 10–200 Å. **Figure 2** is the SEM cross-sectional view of a 20-layer Si/SiO_2 nanostructure comprising 2.0 nm Si and 2.1 nm SiO_2. It shows 20 pairs of the white thin SiO_2 layers and dark Si layers.

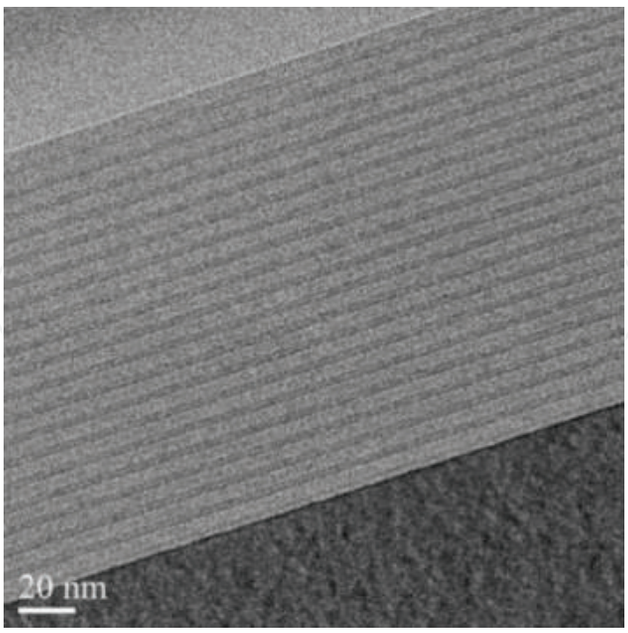

Figure 2. A cross-sectional view of an SEM photograph for an as-deposited 20-layer amorphous Si/SiO_2 film deposited on a fused quartz substrate.

2.1.1. Crystallinity

The XRD spectra (CuKα source) of 180-nm thick Si single layer and 150-nm thick SiO_2 single layer prepared on the sapphire substrates at room temperature do not show the crystallinity of the samples. Both spectra reveal the noncrystalline characteristics of Si and SiO_2 films.

2.1.2. Density-of-states structures

Atomic constitutions of each layer are evaluated with XPS on binding energy of Si2p and O1s electrons. The bulk Si2p core-level binding energy for Si(111) is ~99.3 eV and the bulk Si2p oxide binding energy value for SiO_2 is ~103.7 eV referring to Keister [66]. PHI 500 Versa Probe II scanning XPS microprobe is designed to take out a 10-degree signal, enable slow speed (0.01 nm/s SiO_2) area etching, and equipped with a monochromatic AlKα X-ray source. The depth profiles are characterized by using a low-energy argon ion gun to avoid selective etching. The binding energy dependence of the core densities of states at each etched depth suggests periodic distributions of each atomic composition. This analytical technique has particular applicability to the evaluation of the density of states with atomic contributions. **Figure 3(a)** is the plot of the density of states from 97 to 107 eV as the parameters of depth. The profiles of two peaks (a) 98.9 eV Si 2p spectra (Si^0) (element: un-oxidized) and the 103.2 eV Si 2p (oxidized) (Si^{4+}) are shown. In **Figure 3(b)**, 532.6 eV O1s single peaks are shown. The spectra (a) 103.2 eV and (b) 532.5 eV exhibit maxima at the same depth and spectrum (a) has a minimum at the bottom of (b). **Figure 3(a)**, at the depth of 0.54 nm, 103.2 eV intensity peaks and 98.9 eV show a minimum. The density-of-states depth profiles explain the presence of the Si/SiO_2-layered amorphous nanostructure fabricated using the UHV RF magnetron sputtering method at the atomic scale precision.

2.2. Optical properties of Si/SiO_2 layer films

Optical transmittance spectra and reflectance spectra are measured with the help of JASCO V-670 visible and ultraviolet optical photometer at room temperature. Optical properties of an

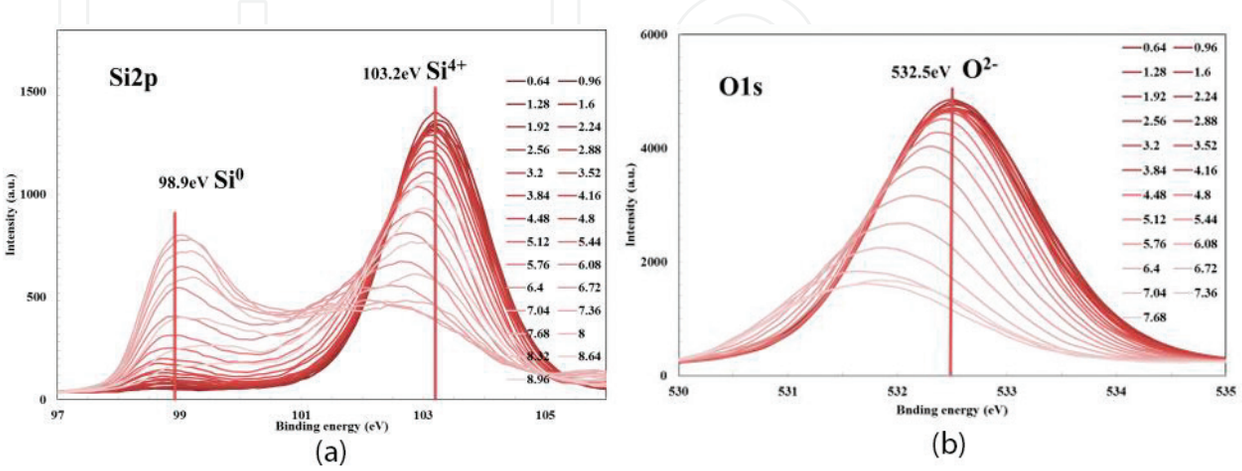

Figure 3. The density-of-states intensity of nanostructure Si/SiO_2 amorphous films. (a) Si2p 99.1 eV (elemental Si) and Si 2p 103.3 eV (oxidized Si) and (b) O1s 532.6 eV.

amorphous Si/SiO_2 nanostructure film show the higher optical transmittance and wide optical window effects. Unique optical properties are a candidate for solar windows in solar cells or filters of ultraviolet light. The parameters characterizing the Si/SO_2 film structures are the well layer thickness, the barrier layer thickness, and the number of periodicity. **Figure 4** displays the optical reflectance and transmittance spectra of amorphous Si/SiO_2-nanostructured layer films of various period numbers. The well thickness of the samples changes from 2 to 24 nm, while the barrier thickness is fixed at 4.8 nm. As the period's number of layers increases, the optical reflection decreases and the optical transmittance increases markedly, although the onset energy of transmittance and the absorption edge wavelength show the constant values. The increasing period number enhances optical transmittance and decreases optical reflectance. The spectra are saturating at 8–12 barrier layers. Increasing the period number does not change the absorption edge energy. Nanostructure effects observed on the 12-layer Si/SiO_2 film as the optical transmittance and reflectance effects are saturating. **Figure 5** exhibits the optical reflectance (a) and transmittance spectra (b) of Si/SiO_2 films as a function of the Si well thickness at the constant 12-period numbers and the constant barrier thickness of 4.8 nm. The increasing Si well thickness increases the reflectance and decreases the transmittance as expected. Also, the absorption edge energy shows the constant values. **Figure 6** shows the barrier thicknesses dependence of optical reflectance (a) and optical transmittance (b) spectra for the constant 12-layer period and 2 nm well thicknesses. The increasing barrier thicknesses diminish the optical reflectance and enhance the optical transmittance.

2.2.1. Absorption coefficient

Absorption coefficients α (λ) are used as the index of intrinsic properties of thin film materials. Absorption coefficient α (λ) at a wave length λ is evaluated from Eq. (1) for the sample thickness d with the optical transmittance T(λ) and reflectance R(λ). On the Si/SiO_2 nanostructure multilayer films, the integrated thickness of the Si layer, the reduced film thickness in Eq. (2) is used as the tentative thicknesses.

$$T = \frac{(1-R)^2 \exp(-\alpha d)}{1-R^2 \exp(-2\alpha d)} \tag{1}$$

$$d = \sum_{i=0}^{n} d_i \tag{2}$$

$$(\alpha h\nu)^{1/2} = \beta(h\nu - E_0) \quad \alpha > 10^3 \tag{3}$$

Figure 7 shows the dependence of the absorption coefficients on the Si well thickness of 12-layer Si/SiO_2 films. The photon energy dependences of absorption coefficient show a sharp rise in the energy of absorption edges above 1000/cm. The dependence of the absorption edge energies on the Si well layer thickness is measured from 0.5 to 6 nm at the SiO_2 barrier layer fixed at 2.4 nm. In **Figure 8**, $(\alpha h\nu)^{1/2}$ vs. photon energy is plotted. The absorption coefficients of amorphous films are related in Eq. (3) known as an amorphous plot to obtain the absorption edge energy.

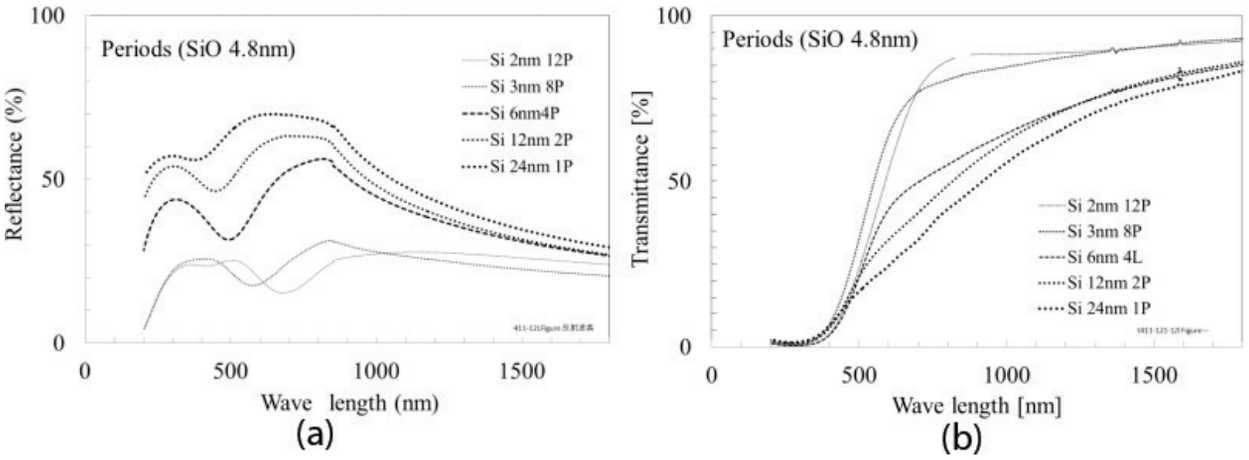

Figure 4. Optical properties of amorphous Si/SiO_2 multilayer films at the constant barrier thickness and the constant integrated well thicknesses as a function of the layer number. (a) Optical reflectance spectra, (b) optical transmittance spectra.

2.2.2. Quantum confinement

In **Figure 9**, the absorption edge energy is plotted vs. the tentative well thicknesses in a Si/SiO_2 multilayer structure and compared with the effective-mass theoretical estimations. Two types of the absorption edge energy evaluated from **Figures 7** and **8** are indicated. The absorption edge energy becomes larger as the QW thickness gets smaller. The blue shifts of the absorption energy are impressive in **Figure 9**. The absorption edge energy values E_0 are evaluated for each well thickness following the effective-mass theory, Eq. (4) [9]. The Si layer thickness dependency of absorption edge energy is in accordance with the effective-mass theory for thicknesses $0.5 < d < 6$ nm in Eq. (4). Therefore, a good agreement is obtained with the effective mass theory assuming infinite potential barriers [34]. The thickness variation of the absorption edge energy shown in **Figure 9** demonstrates a remarkable blue shift of the spectra as the Si layer thickness decreases. This shift can only be caused by the Si layer because the SiO_2 barrier layer thickness is a constant value of 4.8 nm. This absorption edge energy is in accordance with E_0 (eV) = 1.61 + 0.75 d^{-2} (eV).

$$E_0 = Eg + \frac{\hbar^2 \pi^2 n^2}{2 m_0 d^2}\left(\frac{1}{m_e} + \frac{1}{m_h}\right) = E_g + \frac{0.75}{d^2}\,(\text{eV}) \quad \left(d:\text{nm},\, m_e = 1,\, m_h = 1\right) \tag{4}$$

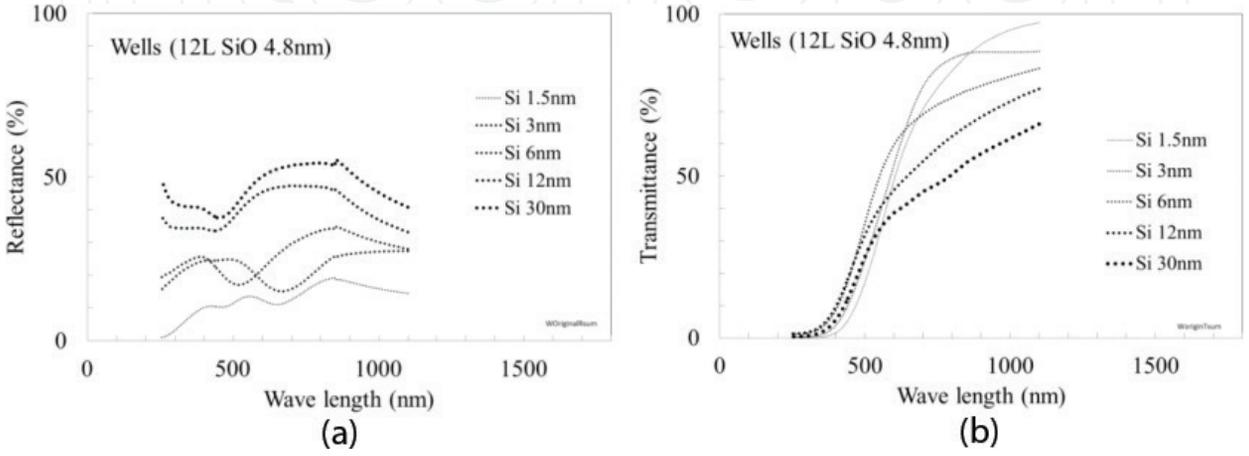

Figure 5. Optical properties of 12-layer Si/SiO_2 films of different QW thicknesses. The barrier thickness is 4.8 nm. (a) Optical reflectance spectra, (b) optical transmittance spectra.

http://dx.doi.org/10.5772/intechopen.79880

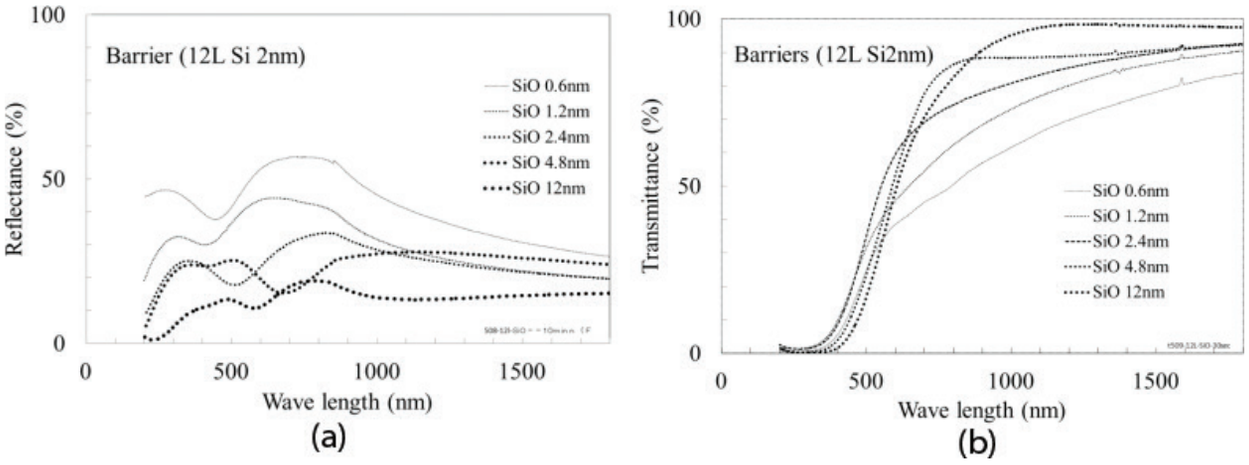

Figure 6. Optical properties of a 12-layer Si/SiO_2 film at a constant QW thickness of 2 nm for different barrier thicknesses. (a) Optical reflectance, (b) optical transmittance.

Although quantum confinement is obtained from the optical absorption measurements, the recombination mechanism is still indistinct. To elucidate the latter, we investigate PL spectra of the Si/SiO_2 multilayer nanostructures.

2.3. Thermal annealing of Si/SiO_2 layer films

Since the as-deposited samples show very weak photoluminescence, two experimental efforts are made to improve the PL intensity. The first is the increasing the well number of Si/SiO_2 films layered with 0.5–15 nm (Si) QWs from 10 to 50 periods. The second is the thermal annealing of Si/SiO_2 films in nitrogen. In our work, RTA in nitrogen was performed at 700 and 1100°C for 30 min. **Figure 10** shows the cross-sectional view of an RTA treated Si/SiO_2 film. Apparently, the Si QW layers are changed revealing partially dark spots and eroded SiO_2 barrier layers.

Figure 11 shows the XRD spectra of a 10-layer Si/SiO_2 film on a sapphire substrate which is rapid-thermal annealed at 700 and 1100°C. The crystallization is clearly identified at 700°C by the splitting the (111), (220), and (311) Braggs peaks indicating that the amorphous Si layers are crystallized as the nanocrystal Si.

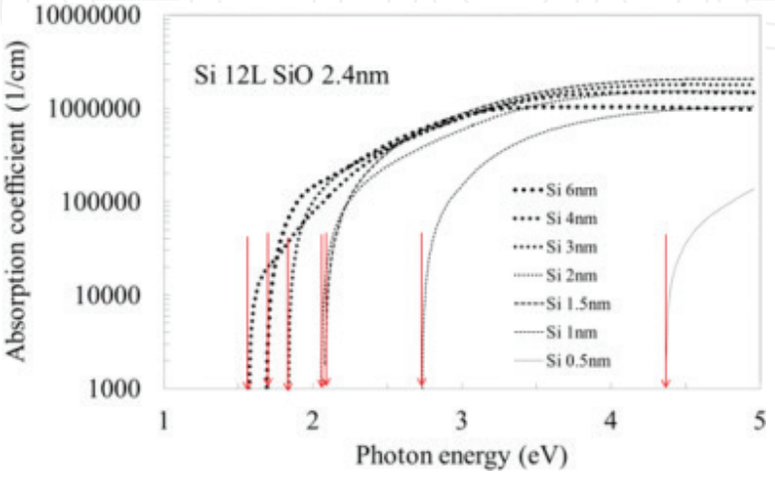

Figure 7. Absorption coefficient spectra for a 12-layer Si/SiO_2 film with a 2.4-nm SiO_2 barrier for different thicknesses of the Si well layer.

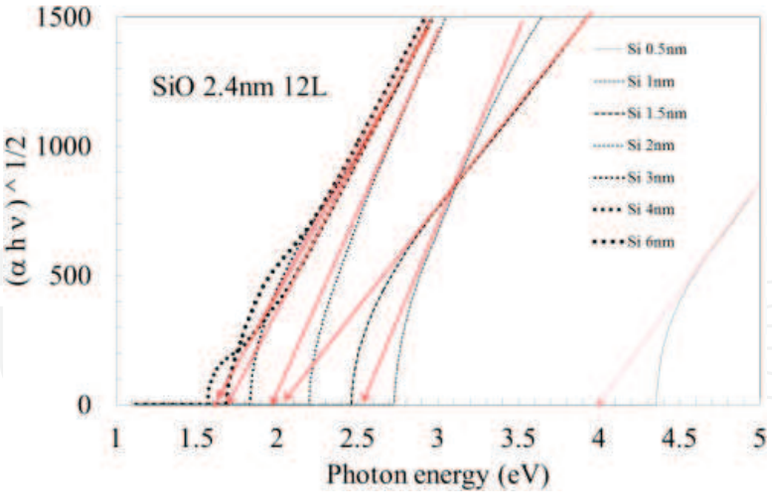

Figure 8. An enlarged view of absorption coefficient spectra displayed in **Figure 7**. The extrapolation gives the optical band gap energy.

2.3.1. Photoluminescence of Si/SiO$_2$ layer films

Photoluminescence spectra of as-deposited amorphous 10 layers Si/SiO$_2$ films are excited at 325 nm by a He-Cd laser. The highest energy peaks at 2.35, 2.05, 1.81 eV, with subpeak at 1.45 eV are observed. The improved PL is observed upon crystallization of Si after subjecting the 50-layer Si/SiO$_2$ multilayer nanostructures to RTA at 700 and 1100°C as shown in **Figure 12**. The spectra show a broadband peak and shoulders. The main peak energies are 1.62, 1.68, and 1.45 eV. In **Figure 13**, photoluminescence spectra of Si/SiO$_2$ QWs annealed at 1100°C for 30 min in nitrogen are shown for the QW thickness ranging from 1.2 to 2.5 nm. The intensity becomes higher for the thinner QWs.

Figure 13 presents the well thickness dependence of PL spectra taken on the 50-layer Si/SiO$_2$ structure upon RTA in nitrogen at 1100°C. The strongest PL is observed for the thinnest Si QW (1.2 nm), fading as the QW thickness increases. **Figure 14** displays the temperature dependences of photoluminescence spectra. Among the three temperatures, the 80 K spectrum is the

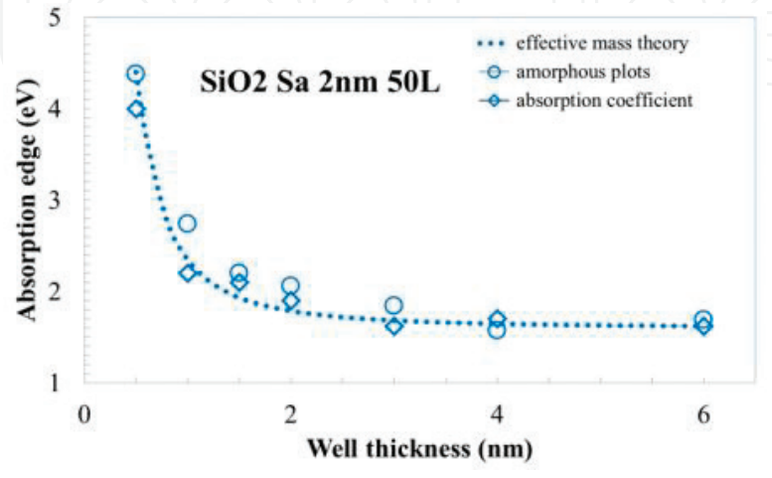

Figure 9. The absorption edge energy as a function of the QW thickness at the constant 2.4-nm SiO$_2$ barrier thickness in a Si/SiO$_2$ multilayer structure.

http://dx.doi.org/10.5772/intechopen.79880

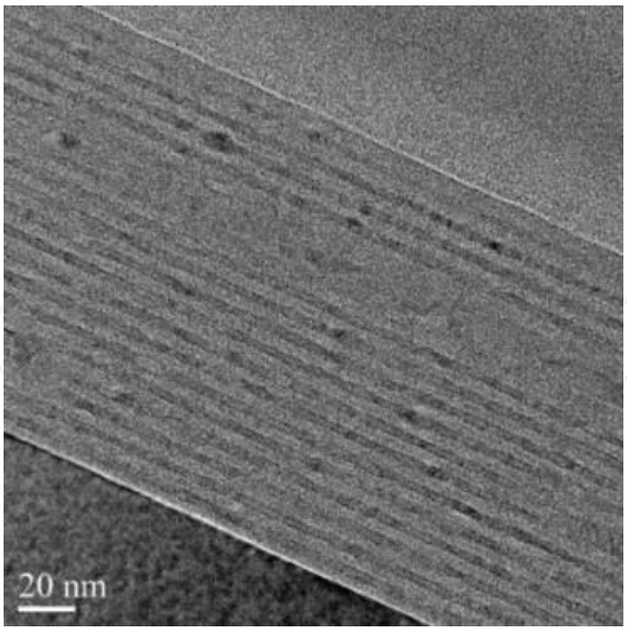

Figure 10. A cross-sectional view of SEM on an amorphous Si/SiO_2 film rapid thermal annealed at 1100°C in nitrogen.

most intense, followed by the room temperature, and the 4 K photoluminescence. The Kapoor model, where two different recombination mechanisms are operative in different temperature ranges, can explain this nonmonotonous temperature dependence of PL. The Kapoor's Eq. (5) consists of an Arrhenius-type term T_r and a Berthelot term T_B. Rolver explained the effects as an interplay of thermal activation of excitons into optically active states and hopping occupation of dark states.

$$I(T) = \frac{I_0}{1 + v_o \exp\left[\left(\frac{T}{T_B} + \frac{T_r}{T}\right)\right]} \tag{5}$$

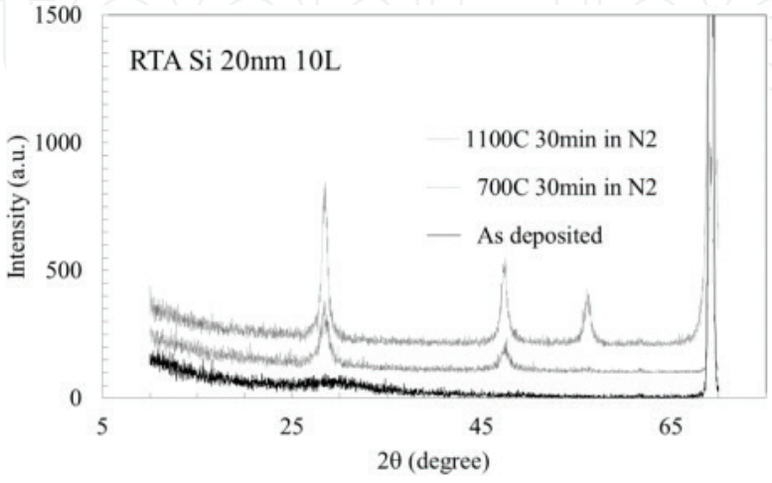

Figure 11. XRD spectra of a Si/SiO_2 multilayer nanostructure grown on a sapphire substrate and rapid-thermal annealed at 700 or 1100°C.

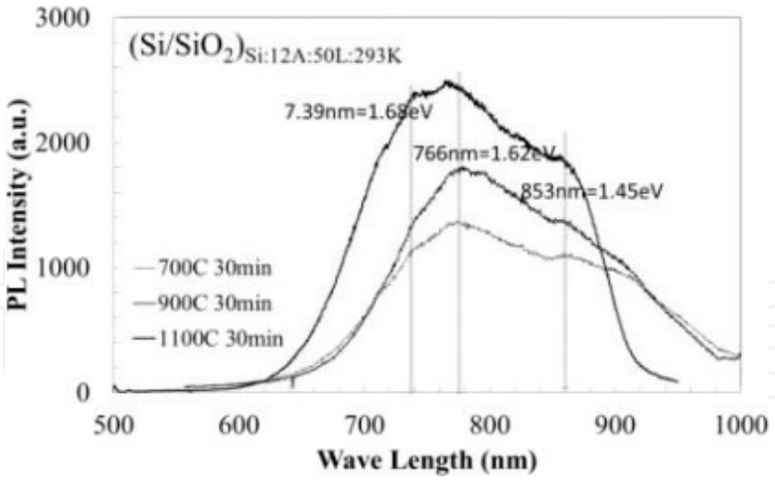

Figure 12. PL spectra of Si/SiO_2 QWs and annealing effects on the photoluminescence intensity of the 50-layer Si/SiO_2 (1.2 nm Si and 2.4 nm SiO_2) structures at room temperature.

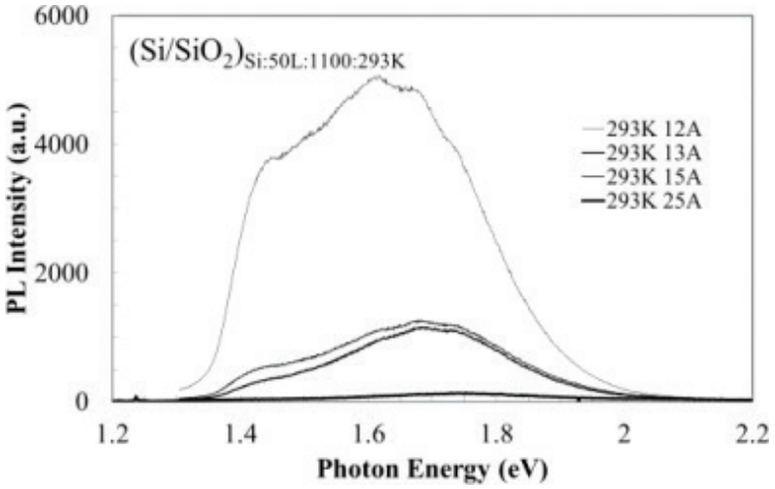

Figure 13. PL spectra of the 50 L Si/SiO_2 of different QW thicknesses (1.2, 1.3, 1.5, and 2.5 nm) annealed at 1100°C.

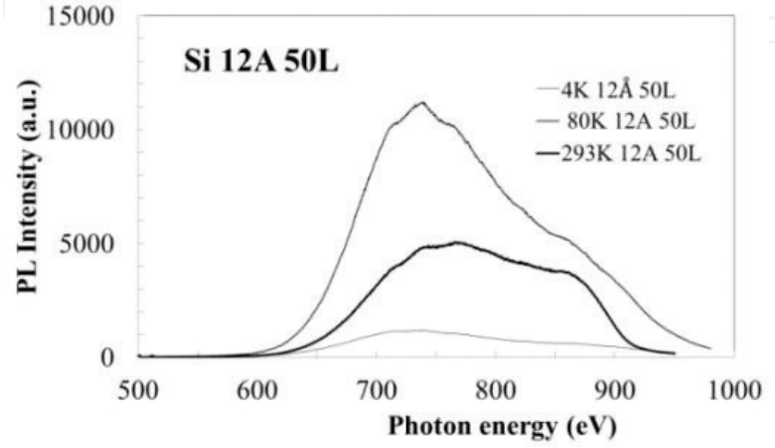

Figure 14. Temperature-dependent PL spectra. Intensity increases from 4 to 293 K and 80 K.

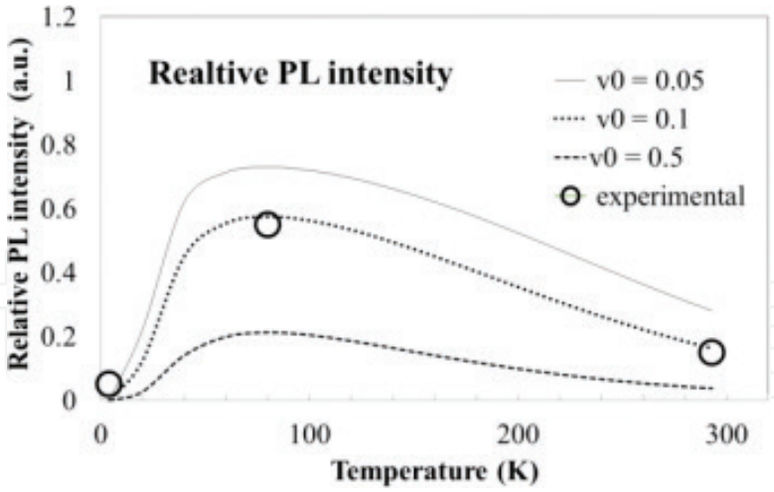

Figure 15. Temperature dependences of the PL peak intensity following the Kapoor model. The experimental results are consistent with the theory.

2.3.2. The Kapoor model

The temperature dependence of the photoluminescence intensity peaks observed at 80, 4, and 293 K are analyzed using the Kapoor empirical models [45, 67]. The simulation of the Si/SiO_2 sample comprising 50 quantum wells (1.2 nm well width) annealed at 1100°C for 30 min in nitrogen is performed following Eq. (5). **Figure 15** presents the result, which evidences a reasonable agreement between the experimental and simulated results using $T_r = 70$ K, $T_B = 80$ K, and $\upsilon_0 = 0.1$.

3. Summary

Amorphous nanostructured Si/SiO_2 films are smartly fabricated using a UHV RF magnetron sputtering system at room temperature. Absorption coefficients are evaluated considering the tentative well Si thickness and energy band gap energy of the Si/SiO_2 layers. The photon energy dependence of absorption coefficient on the quantum well thickness is simulated taking into account the quantum-confined properties. The choice of the Si layer thicknesses interfacing the SiO_2 barrier layer of the constant thickness (4.8 nm) mainly determines the blue shift of the absorption energy. Assuming the infinite potential SiO_2 barriers, the effective-mass theory provides the fitted absorption coefficient edge energy in accordance with $E\ (eV) = 1.61 + 0.75\ d^{-2}\ (eV)$ for one-dimensionally confined amorphous Si (d: nm). The amorphous Si/SiO_2 nanostructure films show the quantum confinement. Thermal annealing of the Si/SiO_2 films affects the improvement of photoluminescence intensity. Anomalous temperature dependence of photoluminescence is attempted to be explained based on the Kapoor model. Future work is expected to resolve many more research questions.

Acknowledgements

The authors express deep thanks to Mr. Minoru Kondo, a graduate student of Waseda University, for corporate experimental works and to Dr. Atsushi Kawaharatsuka, Associate Professor of

Waseda University, for many impressive discussions on quantum confinement. One of the authors (T. T.) expresses deep thanks to Dr. Tadashi Takahashi, Emeritus Professor at Tohoku University, for his encouragements and instructions.

Author details

Toshio Takeuchi[1]* and Yoshiji Horikoshi[2]

*Address all correspondence to: toshio-takeuchi@ve.cat-v.ne.jp

1 Sendai National College of Technology, Sendai, Japan

2 School of Science and Engineering, Waseda University, Tokyo, Japan

References

[1] Ley L, Kowalczyk S, Pollak R, Shirley DA. X-ray photoemission spectra of crystalline and amorphous si and ge valence bands. Physical Review Letters. 1972;**29**:1088-1092

[2] Abeles B, Tiedje T. Amorphous semiconductor superlattices. Physical Review Letters. 1983;**51**:2003-2006

[3] Tiedje T, Abeles B, Brooks BG. Energy transport and size effects in the photoluminescence of amorphous-germanium/amorphous-silicon multilayer structures. Physical Review Letters. 1985;**54**:2545-2548

[4] Wilson BA, Taylor CM, Harbison CM. Photoluminescence in ultrathin a-Si:H layers. Physical Review B. 1986;**34**:8733-8739

[5] Yang L, Abeles B. Quantum shift of the optical absorption edge in ultrathin amorphous hydrogenated germanium. Applied Physics Letters. 1987;**51**:264-266

[6] Miyazaki S, Ihara Y, Hirose M. Resonant tunnelingthrough amorphous silicon-silicon nitride double barrier structures. Physical Review Letters. 1987;**59**:125-127

[7] Kalm S. Optical investigation of a-Si:H/a-SiNx:H superlattice. Physical Review B. 1988;**37**: 8837-8841

[8] Hattori K, Mori T, Okamoto H, Hamakawa Y. Optical observation of subbands in amorphous silicon ultrathin single layers. Applied Physics Letters. 1988;**53**:2170-2172

[9] Yang L, Abeles B, Eberhardt W, Stasiewski H, Sondericker D. Photoemission spectroscopy of heterojunctions of hydrogenated amorphous silicon with silicon oxide and nitride. Physical Review B. 1989;**39**:3801-3815

[10] Lockwood DJ. Optical properties of porous silicon. Solid State Communications. 1994;**92**: 101-112

[11] Kovalev D, Pollisski G, Ben-Chorin MM, Diener J, Koch F. The temperature dependence of the absorption coefficient of porous silicon. Journal of Applied Physics. 1996;**89**:5978-5983

[12] Mulloni V, Chierchia R, Mazzoleni C, Pucker G, Pavesi L. Porous silicon optical devices and Si/SiO_2 quantum wells :recent results. Philosophical Magazine. 2000;**80**:705-718

[13] Kanemitsu Y, Okamoto S. Visible luminescence from silicon quantum dots and wells. Materials Science and Engineering. 1997;**B48**:108-115

[14] Kanemitsu Y, Fukunishi Y, Iiboshi M, Okamoto S, Kushida T. Visible luminescence from Si/SiO_2 quantum wells and quantum dots: confinement and localization of excitons. Physics E. 2000;**7**:456-460

[15] Moskalenko AS, Berakdar J, Prokofiev AA, Yassievch IN. Single-particle states in spherical Si/SiO_2 quantum dots. Physics Review. 2007;**76**:08547-1~7

[16] Aberle AG, Glunz SW, Stephens AW, Green MA. High efficiency silicon solar cells: Si/SiO_2 interface parameters and their impact on device performance. Progress in Photovoltaic Research and Application. 1994;**2**:265-273

[17] Kim DH. Current-voltage characterization of silicon quantum dot solar cells. Transactions on Electrical and Electronic Materials. 2009;**10**:143-145

[18] Filikhin I, Matinyan SG, Schmid BK, Vlahovic B. Electronic and level statistics properties of Si/SiO_2 quantum dots. Physics E. 2010;**42**:1979-1983

[19] A-Ameer NM, Abdulrida MC. Direct optical energy gap in amorphous silicon quantum dots. International Journal of Modern Physics. 2011;**2**:1530-1537

[20] Okamoto S, Kanemitsu Y. Quantum confinement and interface effects on photoluminescence from silicon single quantum wells. Solid State Communications. 1997;**103**:573-576

[21] Kanemitsu Y. Excitons in silicon quantum structures. Journal of Luminescence. 1999;**83-84**: 283-290

[22] Kanemitsu Y, Iiboshi M, Kushida T. Photoluminescence spectrum of a-Si/SiO_2 and c-Si/SiO_2 quantum wells. Journal of Luminescence. 2000;**87-89**:463-465

[23] Kanemitsu Y, Iiboshi M, Kushida T. Photoluminescence dynamics of amorphous Si/SiO_2 quantum wells. Applied Physics Letters. 2000;**76**:2200-2202

[24] Kanemitsu Y. Efficient light emission from crystalline and amorphous silicon nanostructures. Journal of Luminescence. 2002;**100**:209-217

[25] Guha S, Qadri SB, Musket RG, Wall MA, Shimizu-Iwayama T. Characterization of Si nanocrystalline grown by annealing SiO_2 films with uniform concentrations of implanted Si. Journal of Applied Physics. 2000;**88**:3954-3961

[26] Lu ZH, Grozea D. Crystalline Si/SiO_2 quantum wells. Applied Physics Letters. 2002; **80**:255-257

[27] Lockwood DJ, Lu ZH, Grozea D. Photoluminescence in crystalline-Si/SiO_2 quantum wells. Proceeding of SPIE. 2002:**4808**:40-44

[28] Mangolini I, Thimsen E, Kortshagen U. High-Yield Plasma Synthesis of Luminescent Silicon Nanocrystals. Nano Letters. 2005;**5**:655-659

[29] Schubert EF, Vredenberg AM, Hunt NE, Wong YH, Becker PC, Poate JM, Jacobson DC, Feldman LC, Zydzik GJ. Giant enhancement of luminescence intensity in Er-doped Si/SiO_2 resonant cavities. Applied Physics Letters. 1992;**61**:1381-1383

[30] Watanabe K, Fujii M, Hayashi S. Resonant excitation of Er3+ by the energy transfer from Si nanocrystals. Journal of Applied Physics. 2001;**90**:4761-4767

[31] Gourbilleau F, Dufour C, Madelon R, Rizk R. Spectroscopic studies of Er-doped Si-rich oxide/SiO_2 multilayers. Optica Applicata. 2007;**37**:21-29

[32] Lu ZH, Lockwood DJ, Barbeau JM. Quantum confinement and light emission in SiO_2/Si superlattices. Nature. 1995;**378**:258-260

[33] Vervoot L, Bassani F, Mihalceescu I, Vial JC, Davitani FA. Efficient visible-light emission from Si/SiCaF2(111) heterostructures grown by molecular beam epitaxy. Physica Status Solidi. 1955;**190**:123-127

[34] Lockwood DJ, Lu ZH, Barbeau JM. Quantum confinement luminescence in Si/SiO_2 superlattices . Physical Review Letters. 1996;**76**:539-541

[35] Lu ZH, Lockwood DJ, Barbeau JM. Visible light emitting Si/SiO_2 superlattices. Solid-State Electronics. 1996;**40**:197-201

[36] Tsu R, Filios A, Lofgren C, Cahill D, Vannostrand J, Wang CG. An epitaxial Si/SiO_2 superlattice barrier. Solid State Electronics. 1996;**40**:221-223

[37] Khriachtchev L, Kilpela O, Karirinne S, Keranen J, Lepisto T. Substrate-dependent crystallization and enhancement of visible photoluminescence in thermal annealing of Si/SiO_2 superlattices. Applied Physics Letters. 2001;**78**:323-325

[38] Nassiopoulou AG, Ioannou-Sougleridis V, Photopoulos P, Travlos P, Tsakiri V, Paradimitriou D. Stable visible photo- and electroluminescence from nanocrystalline silicon thin films fabricated on thin SiO_2 layers by low pressure chemical vapor deposition. Physica Status Solidi, (a). 1998;**165**:79-85

[39] Heikkila L, Kuusela T, Hedman HP, Ihantola H. Electroluminescent SiO_2/Si superlattices prepared by low pressure chemical vapor deposition. Applied Surface Science. 1998;**133**:84-88

[40] Tsybeskov L, Hirchman KD, Duttaguta SP, Zacharias M, Fauchet PM, McCaffrey JP, Lockwood DJ. Nanocrystalline-silicon superlattice produced by controlled recrystallization. Applied Physics Letters. 1998;**72**:43-45

[41] Vinciguerra V, Franzo G, Priolo F, Lacona F, Spinella C. Quantum confinement and recombination dynamics in silicon nanocrystals embedded in Si/SiO_2 superlattices. Journal of Applied Physics. 2000;**87**:8165-8172

[42] Park N, Choi C, Seong T, Park S. Quantum confinement in amorphous silicon quantum dots embedded in silicon nitride. Physical Review Letters. 2001;**86**:1355-1357

[43] Arguirov T, Mchedlidze T, Arguirova SK, Kitter M. Light induced solid-phase crystallization of Si nanocrystals in Si/SiO_2 multiple quantum wells. Journal of Applied Physics. 2002;**107**:124302-124309

[44] Wang XX, Zhang JG, Ding L, Cheng BW, Ge WK, Yu JZ, Wang QM. Origin and evolution of photoluminescence from Si nanocrystals embedded in a SiO_2 matrix. Physical Review B. 2005;**72**:195313-1~6

[45] Rolver KR, Fost M, Winkler O, Spangenberg B, Kurz H. Influence of excitonic singlet-triplet splitting on the photoluminescence of Si/SiO_2 multiple quantum wells fabricated by remote plasma-enhanced chemical-vapor deposition. Journal of Vacuum Science and Technology A. 2006;**24**:141-145

[46] Arguirov T, Mchedlidze T, Akhmetov VD, Arguirova SK, Kitter M, Rover R. Berghoff B, Forst M, Batzner DL, Spangenberg S. Effect of laser annealing on crystallinity of the Si layers in Si/SiO_2 multiple quantum wells. Applied Surface Science. 2007;**254**:1083-1086

[47] Bergfoff B, Forst M, Batzner DL, Spangenberg S. Electronic band gap of Si/SiO_2 quantum wells: Comparison of ab initio calculation and photoluminescence measurements. Applied Surface Science. 2007;**254**:1083-1086

[48] Arguirov T, Mchedlidze T, Arguirova SK, Kitter M, Rover R, Berghoff B, Batzner D, Spangenberg S. Laser annealing of the Si layers in Si/SiO_2 multiple quantum wells. Materials Science and Engineering B. 2009;**159-160**:57-60

[49] Puglisi RA, Vecchio C, Lombardo S, Lorenti S, Camallen MC. Charge transport in ultrathin silicon rich oxide/SiO_2 multilayers under solar light illumination and in dark conditions. Journal of Applied Physics. 2010;**108**:023701-1~7

[50] Kanzawa Y et al. Size-dependent near-infrared photoluminescence spectra of Si nanocrystals embedded in SiO_2 matrices. Solid State Communications. 1979;**102**:533-537

[51] Zayats AV, Yu A, Repeyev A, Nikogosyan DN, Vinogrado EA. Radiative recombination in short-period a-Si/SiO_2 superlattices. Journal of Luminescence. 1972;**52**:335-343

[52] Dobrowolski JA, Pekelsky JR, Pelletier R, Ranger M, Sullivan B, Waldolf AJ. Practical magnetron sputtering system for the deposition of optical multilayer coating. Applied Optics. 1992;**31**:3784-3789

[53] Sullivan B, Dobrowolski JA. Applied Optics. Deposition error compensation for optical multilayer coating. II. Experimental Results-Sputtering System. 1993;**32**:2351-2360

[54] Sullivan B, Byrt KL. Metal/dielectric transmission interference filters with low reflectance. 2. Experimental results. Applied Optics. 1995;**34**:5684-5694

[55] Zacharias M, Tsybeskov L, Hirschman KD, Fauchet PM, Blasing J, Veit P, Blasting J, Kohlert P, Veit P. Nanocrystalline silicon superlattices: Fabrication and characterization. Journal of Non-Crystalline Solids. 1998;**227-230**:1132-1136

[56] Qin GG, Ma SY, Ma ZC, Zong WH, Liping Y. Electroluminescence from amorphous Si/SiO_2 superlattices. Solid State Communications. 1998;**106**:329-333

[57] Zacharias M, Blasing J, Veit P, Tsybeskov L, Hirschman K, Fauchet PM. Thermal crystallization of amorphous Si/SiO_2 superlattices. Applied Physics Letters. 1999;**74**:2614-2616

[58] Zacharias M, Streitenberger P. Crystallization of amorphous superlattice in the limit of ultrathin films with oxide interfaces. Physical Review B. 2000;**62**:8391-8396

[59] Benyoucef M, Kuball M, Sun JM, Zhong GZ, Fan XW. Raman scattering and photoluminescence studies on Si/SiO_2 superlattices. Journal of Applied Physics. 2001;**89**:7903-7907

[60] Cho EC, Xia J, Aberle AG, Green MA. Antireflection and surface passivation behavior of SiO_2/Si/SiO_2 quantum wells on Si. Solar Energy Materials & Solar Cells. 2002;**74**:147-154

[61] Tenron C, Gourbilleau F, Rizk R, Dufour C. Si/SiO_2 multilayers: synthesis by reactive magnetron sputtering and photoluminescence emission. Physica E. 2003;**16**:517-522

[62] Hanaizumi O, Ono K, Ogawa Y. Blue-light emission from sputtered Si:SiO_2 films without annealing. Applied Physics Letters. 2003;**82**:538-540

[63] Portier X, Ternon C, Gourbilleau F, Dufour C, Rizk R. Anneal temperature dependence of Si/SiO_2 superlattices photoluminescence. Physica E. 2003;**16**:439-444

[64] Huang S, Xiao H, Shou S. Annealing temperature dependence of Raman scattering in Si/SiO_2 superlattice prepared by magnetron sputtering. Applied Surface Science. 2009;**255**:4547-4550

[65] Takeuchi T, Kondo M, Fujita M, Kawaharazuka A, Horikoshi Y. Optical properties of amorphous and nanostructured Si/SiO_2 quantum wells. Journal of Nano Research. 2014; **26**:59-62

[66] Keister JW, Rowe JE, et al. Structure of ultrathin SiO_2/Si(111) interface studied by photoelectron spectroscopy. Journal of Vacuum Science and Technology. 1999;**A17**:1250-1257

[67] Kapoor M, Sinh VA, Johri GK. Origin of the anomalous temperature dependence of luminescence in semiconductor nanocrystalline. Physical Review B. 2000;**61**:1941-1945